Journal of Traditional Chinese Medical Sciences (2015) 2, 60–68

HOSTED BY

ELSEVIER

Available online at www.sciencedirect.com

ScienceDirect

journal homepage: http://www.elsevier.com/locate/jtcms

Effect of Chinese tuina massage therapy on resting state brain functional network of patients with chronic neck pain

Hua Zhang [a,1], Hong Chen [b,1], Hao Wang [b], Duoduo Li [b], Baolin Jia [b], Zhongjian Tan [c], Bin Zheng [d,*], Zhiwen Weng [b,*]

[a] *Department of Neurology and Stroke Center, Dongzhimen Hospital, Beijing University of Chinese Medicine, Beijing 100700, China*
[b] *Department of Massage, Dongzhimen Hospital, Beijing University of Chinese Medicine, Beijing 100700, China*
[c] *Department of Radiology, Dongzhimen Hospital, Beijing University of Chinese Medicine, Beijing 100700, China*
[d] *Department of Traditional Chinese Medicine, Beijing Chaoyang Hospital, Capital Medical University, Beijing 100026, China*

Available online 15 December 2015

KEYWORDS
Chronic pain;
Traditional Chinese tuina;
Resting state network;
Independent component analysis;
Granger causality

Abstract *Objective:* Cervical disease, a type of chronic pain, can greatly impact quality of life. Traditional Chinese tuina, a form of therapeutic massage and manipulation, has been shown to be effective in relieving pain and other symptoms in patients with chronic neck pain. This study applied functional magnetic resonance imaging (fMRI) to explore the features of the resting state network of patients with chronic neck pain caused by cervical radiculopathy, and how tuina affects the causality between intrinsic brain networks.
Methods: Using Granger causality analysis, effective connectivity of brain networks of 10 patients with chronic neck pain was compared with 10 healthy control subjects. Resting state fMRI data were using magnetic resonance scanning. Cervical spondylosis symptom scores were evaluated before and after 4 weeks of tuina therapy. Independent component analysis was applied to extract the specific networks related to sensation, execution, and cognition, including sensorimotor network (SMN), visual network (VN), auditory network (AN), anterior and posterior default mode network (aDMN, pDMN), left frontoparietal network and right frontoparietal network.
Results: Compared with the control group, data from the treatment group revealed two major findings: before tuina therapy, SMN had a profound influence on aDMN and AN greatly affected pDMN; however, after 4 weeks of tuina therapy, aDMN and SMN showed reversed causality.

* Corresponding authors.
E-mail addresses: zhengbin1220@gmail.com (B. Zheng), wengzhiwen2003@aliyun.com (Z. Weng).
Peer review under responsibility of Beijing University of Chinese Medicine.
[1] These authors equally contributed to this work.

http://dx.doi.org/10.1016/j.jtcms.2015.10.001

Conclusion: Chronic neck pain caused by cervical radiculopathy may influence the DMN, which plays an important role in emotion, cognition, and memory, by stimulating the sensory afferent network. Tuina not only significantly relieves pain and discomfort, but also reverses the causality between aDMN and SMN.

Introduction

Chronic pain is defined as pain that lasts at least 3—6 months.[1] It can also be defined as pain that requires more time for tissue healing.[2] Pain is not only a physical illness, but also a psychosomatic disorder. Chronic pain can cause brain dysfunction through complex pathophysiologic mechanisms and lead to mental disorders such as, depression and anxiety, as well as cognitive impairment, all of which can seriously impact quality of life. With increasing duration, chronic pain becomes more difficult to manage.[3] Cervical spine disease is a common cause of chronic pain. In China, cervical radiculopathy comprises 50%—70% of the incidence of cervical disease.[4]

Among non-drug therapies for cervical disease, Chinese tuina is widely used in China. Tuina is a form of traditional Chinese bodywork, or massage therapy. It has a long history in China and is an important part of traditional Chinese medicine. Tuina achieves pain relief through harmonizing the *yin* and *yang* of the organs.[5] Tuina is considered gentle on the body and as such, patients prefer tuina over pharmaceutical drugs. The central mechanism of tuina therapy on cervical radiculopathy is not clear.

Changes in the brain functional network caused by pain can be identified and quantified through the neuroimaging methodology of resting-state functional magnetic resonance imaging (fMRI).[6,7] In the study of brain functional networks, the causality model is better suited to describe intranetwork communication than the functional connectivity model. The Granger causality analysis (GCA) is a commonly used method in research.[8] Goebel et al originally proposed using the self-regression model and the GCA application with fMRI.[9] Deshpande et al utilized the multivariate Granger causality model[10] for tactile sensation functional data generated by fMRI, and identified the top—down network from the sensory cortex to the visual cortex, as well as the top—down network connection from the visual cortex to the parietal lobe. As research on brain functional networks has progressed, the GCA model has expanded from nodes in functional regions of the brain to an established functional network. Londei et al were among the earliest researchers to apply GCA to brain networks identified through independent component analysis (ICA) in fMRI data processing.[11] Combining ICA with GCA, Oguz et al found that the secondary visual network and the cerebellum network are the key nodes connecting multiple brain regions in implementing cognitive, visual, and auditory tasks.[12] Liu et al applied ICA and conditional GCA in resting-state fMRI, and confirmed that the default mode network is the key component in the human brain functional structure, validating the top—down modulation functions of the default mode network (DMN) on the sensory and cognitive aspects of mental activities.[13] With the application of generalized partial directed coherence (GPDC) measurements, Havlicek et al adopted the multivariate autoregressive (MAR) model in frequency domain analysis after isolating related brain networks through ICA, and measured the degree of brain network causality strength in — auditory sensorimotor and auditory recognition activities.[14] In pain research, Bruneau et al explored the causal relationship between the amygdala and the extended pain matrix in the brain through the use of GCA while reading stories to elicit painful and depressing emotions in patients.[15] Leung et al studied the effect of acupuncture needling at the acupoints SP1 and CV2 on heat-induced pain, using GCA measurements.[16] However, there is relatively little research using GCA intranetworks to explore the central mechanisms of chronic pain caused by cervical diseases. This study used ICA to isolate afferent sensory networks and networks related to cognitive implementation, and applied the multivariate Granger model to analyze the intranetwork causality in patients with chronic pain. We focused on the changes in causal relationships before and after Chinese tuina therapy.

Eligibility and methods

Participants

A total of 20 participants were enrolled in the study. Ten participants were patients treated from July 2013 to January 2014 at the Tuina Clinic at the Beijing University of Chinese Medicine Dongzhimen Hospital. The remaining 10 participants were gender and age matched healthy controls recruited from Beijing Dongcheng district. All participants were determined to be right-handed according to the Edinburg Handedness Inventory.[17] This study was approved by the Medical Ethics Committee of Dongzhimen Hospital and all experimental procedures were conducted in accordance with the Declaration of Helsinki. All participants signed informed consent forms.

Inclusion criteria

This study adopted the diagnostic criteria for cervical radiculopathy established by the Third National Symposium of Cervical Spondylosis (China).[18] Diagnosis was based on symptoms, signs, and X-ray, and 20-minute evaluation using Tanaka's 20-point cervical radiculopathy score[19] and the

visual analog scale (VAS) for pain. Patients with depression were excluded using the Hamilton Depression Rating Scale 17-Item (HAMD).[20]

Symptoms and signs considered for inclusion were as follows with numbers 1—4 as inclusion prerequisites:

1) Presence of neck, shoulder, and back pain, stiffness; pain and/or numbness in the upper extremities; region of pain consistent with the cervical dermatome distribution; persistent pain for 6 months or more.
2) Limited neck movement.
3) Tenseness of the posterior neck muscles, with trigger points (tight bands or knots of muscle); tenderness, radiating pain, and numbness may occur on or adjacent to the spinous process, or in the depression between spinous processes and nearby nerves, consistent with the affected cervical dermatome distribution.
4) Positive brachial plexus tension test and/or cervical compression test.
5) Weakness of muscle innervated by the involved nerve root; sense of pain and touch may be reduced.
6) Reduced or absence of tendon reflexes.

One of the following two imaging results was required for inclusion:

1) Plain radiography: normal or loss of normal cervical lordosis, narrowed disc space, vertebral hyperplasia, intervertebral foraminal stenosis, or calcification of ligaments.
2) CT or MRI scanning: vertebral hyperplasia, cervical spinal or nerve root canal stenosis, herniated or bulging disc, ligament hypertrophy, spinal nerve compression.

Intervention: Chinese tuina therapy

All participants in the intervention group received the following tuina therapy:

1. Rolling method, tapping method, plucking method, and kneading method were applied on the neck, shoulders, back, and upper arms.
2. Supine cervical pulling method was applied with intensity adjusted based on the severity of the disease.

For main symptoms of neck, shoulder, and back pain:

Tuina was applied at the following acupoints on the affected side: GB20, GB21, BL13, BL17, BL42, BL44.

For main symptoms of ulnar or palmar side upper arm pain or numbness:

1. Tuina was applied at the following acupoints on the affected side: HT1, HT2, HT3, HT6, SI9, SI8, PC3, PC6.
2. Tuina clench method and arm smoothing method were applied to the following channels, in the same direction as channel flow: Heart, Pericardium, and Small Intestine.

For main symptoms of pain and numbness on the dorsal and the radial sides of the upper arm:

1. Tuina was applied at the following acupoints on the affected side: SJ14, SJ13, LI15, LI13, LI11, LI6, LI5, LI4.
2. Tuina clench method and arm smoothing method were applied to the following channels, in the same direction as channel flow: Large Intestine, Triple Energizer (San Jiao), and Lung.

Each treatment session was 35—40 min and sessions were once every other day, with 12 sessions comprising one course of treatment. The cervical spondylosis symptom scale and VAS and HAMD scales were used to evaluate participants before and after treatment.

Brain functional imaging

MRI scans were performed on the 10 participants in the intervention group 3 days before tuina treatment and within 3 days after completion of all tuina sessions. MRI scans were performed on the 10 healthy controls only once, 3 days before tuina treatment for the intervention group. Magnetic resonance image acquisition was obtained using the Siemens MAGNETOM Verio 3.0T system (Siemens Medical Solutions, Malvern, PA, USA), including three-dimensional structural imaging scans that utilized T1WI sequences to scan the whole brain. Acquisition parameters: layer thickness: 1.0 mm, TR: 1900 ms, TE: 3.93 ms, Fov: 240 $\times$ 240, flip angle: 15°, number of layers: 176 $\pm$ 5.

Resting-state functional magnetic resonance used T2*WI gradient echo—echo planar imaging (EPI) sequences. Acquisition parameters: layer thickness: 3.5 mm, layer spacing: 0.7 mm, TR: 2000 ms, TE: 50 ms, scan matrix: 128 $\times$ 128, Fov: 240 $\times$ 240, flip angle: 90°, number of layers: 26. Two hundred and ten images were collected.

Participants' heads were stabilized using foam pillows to reduce head movement and earplugs were used to reduce noise. Participants were instructed to close their eyes, relax, stay awake, and keep their minds clear.

Data processing

Data were pre-processed using the Data Processing Assistant for Resting-State fMRI (DPARSF) software package (Beijing Normal University, Beijing, China).[21] The original file format was converted to NIfTI-1 data format (Neuroimaging Informatics Technology Initiative, National Institute of Mental Health, Bethesda, MD, USA). To eliminate the influence of magnetic field inhomogeneity, data from 10 prior time points were removed from the resting-state images. After correcting for slice timing and head movement, displacement/angle in the 3 translational directions and the 3 rotational directions were all less than 2 mm/degree. Functional imaging was performed based on the standardized diffeomorphic anatomical registration through exponentiated lie algebra (DARTEL) process that was aligned with the Montreal Neurological Institute (MNI) template and was smoothed with 8 mm full-width at half-maximum (FWHM) Gaussian kernel.

Independent component analysis (ICA) using the Group ICA of fMRI Toolbox (GIFT)[22] software (University of New Mexico, Albuquerque, NM, USA) to perform ICA calculation on all resting-state data. Using the minimum description

length (MDL) technique, the number of independent components in the package was estimated to be 14. To prevent sample order randomness from affecting ICA results, RandInit and Bootstrap operations were repeated 20 times and the 14 components were individually calculated and evaluated using the *t* test. Based on the resting-state brain network template published by the GIFT team, all components were calculated by the regression operation, which selected the Somatomotor Network (SMN), the Auditory Network (AN), the Visual Network (VN), the anterior Default Mode Network (aDMN), the posterior Default Mode Network (pDMN), the Left Frontoparietal Network (LFPN), and the Right Frontoparietal Network (RFPN).

Network causal relationship analysis

Functional network connectivity (FNC) software[23] was applied to analyze network causal relationships. Seven resting-state network components were selected and filtered at 0.01—0.1 Hz and the generalized partial directed coherence (GPDC) was selected as the measured parameter. Between the 0.01—0.1 Hz bandwidth, the multivariate Granger model estimation was utilized. Using group level optimization from the Akaike information criterion (AIC), the order of the model was estimated. To compare the intervention group before treatment with the control group, as well as the intervention group before treatment and after treatment, *P*-values were set as 0.05 for inter- and intra-group comparison. The results were displayed onto a 3D standard brain surface using BrainNet Viewer (Beijing Normal University).[24]

Results

Baseline and post-intervention characteristics of participants

In comparing baseline characteristics between the intervention and control groups, there were no significant differences in age ($P = 0.4095$) and gender ($P = 1.0$) (Table 1). After tuina therapy, the intervention group exhibited significant improvement in cervical spondylosis symptoms, HAMD and VAS scores ($P < 0.001$) (Table 2).

Independent component analysis and statistical results

Group independent component analysis was applied to all 30 data sets (2 scan per participant in the intervention group, and 1 scan each for the healthy controls). Three sensory processing networks and 4 cognitive networks were identified from 14 ICA components employing spatial correlation with Allen's resting state networks templates.[25] The correlation coefficients were 0.52 (sensorimotor network), 0.71 (visual network), 0.55 (auditory network), 0.62 (anterior default mode network), 0.73 (posterior default mode network), 0.46 (left frontoparietal network), and 0.62 (right frontoparietal network). No significant differences were found between the intervention group and control group, nor between pre-treatment and post-treatment in the intervention group. Results of one-sample *t* test of 7 networks on the surface of an ICBM-152 brain rendering[26] ($P < 0.05$, Monte Carlo simulation cluster level correction, 1000 iterations) were displayed (Figs. 1 and 2). Spatial distribution details are presented in Tables 3 and 4.

The Granger causality of the afferent sensory and cognitive network showed very different patterns in pre-treatment intervention participants compared with healthy controls (Fig. 3 left and center panels). In the intervention group, aDMN, SMN, and VN comprised the core networks with more effective connections than others, while pDMN and LFPN were the hubs of causal connection in the control group. Two-sample *t* test results showed that the main difference between the intervention and control groups existed between SMN and aDMN, as well as AN and pDMN (Fig. 3 right panel). These results revealed that sensory networks including SMN and AN affected DMN more markedly in low frequency (0.012 Hz and 0.014 Hz) of untreated participants with chronic neck pain than healthy controls.

The one-sample *t* test of intra-group Granger causality analysis in the intervention group showed that after tuina treatment the value of causality and frequency from SMN to aDMN were decreased (Fig. 4 left and center panels). The number of VN causality connections was also reduced from 5 to 3. The causality direction was reversed between LFPN and pDMN which was similar in the control group (Fig. 3 center panel). The paired t test result between pre-treatment and post-treatment confirmed the reversion of causality from SMN to aDMN (Fig. 4 right panel).

Table 1 Baseline characteristics of intervention and control groups.

Groups	Gender (M/F)	Age (y)	Disease duration (y)
Intervention (n = 10)	2/8	50.8 ± 5.4[a]	7.3 ± 5.1[a]
Control (n = 10)	2/8	48 ± 9.8[a]	—

[a] Values expressed as mean (SD).

Table 2 Changes in cervical spondylosis, depression, and pain symptoms in intervention group before and after tuina therapy.

Intervention group	Cervical spondylosis score[a]	HAMD[a]	VAS[a]
Before treatment	12.3 ± 2.4	9.6 ± 2.0	7.1 ± 0.7
After treatment	18.2 ± 1.0[b]	5.5 ± 2.2[b]	2.4 ± 0.7[b]

Abbreviations: HAMD, Hamilton Rating Depression Scale; VAS, visual analog scale for pain.
[a] Values expressed as mean (SD).
[b] $P < 0.001$.

Discussion

The sensing of pain is a complex physiological and psychological activity, involving integration of exogenous and endogenous information, and shares multiple core brain

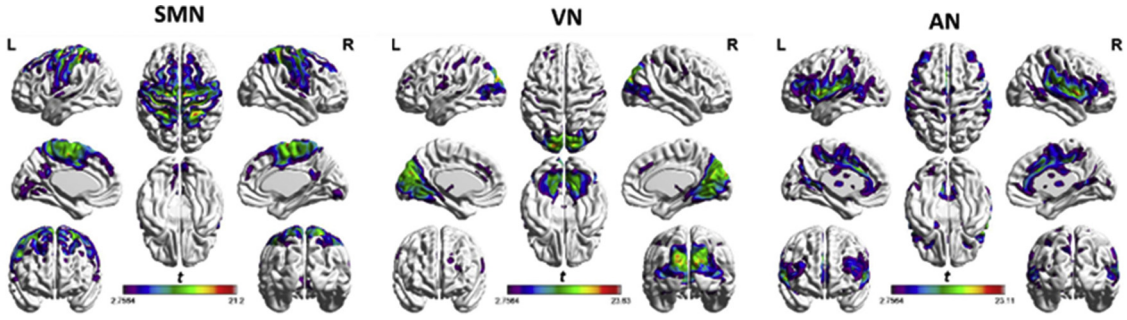

Figure 1 Afferent sensory network screened through ICA.
One-sample *t* test of afferent sensory network of all 30 participants projected onto ICBM-152 brain surface template, as identified through ICA, including sensorimotor network (SMN), visual network (VN), and audio network (AN). The *t* value (depicted by cold to warm colors) represents the spatial statistical significance of the current network. L, left; R, right.

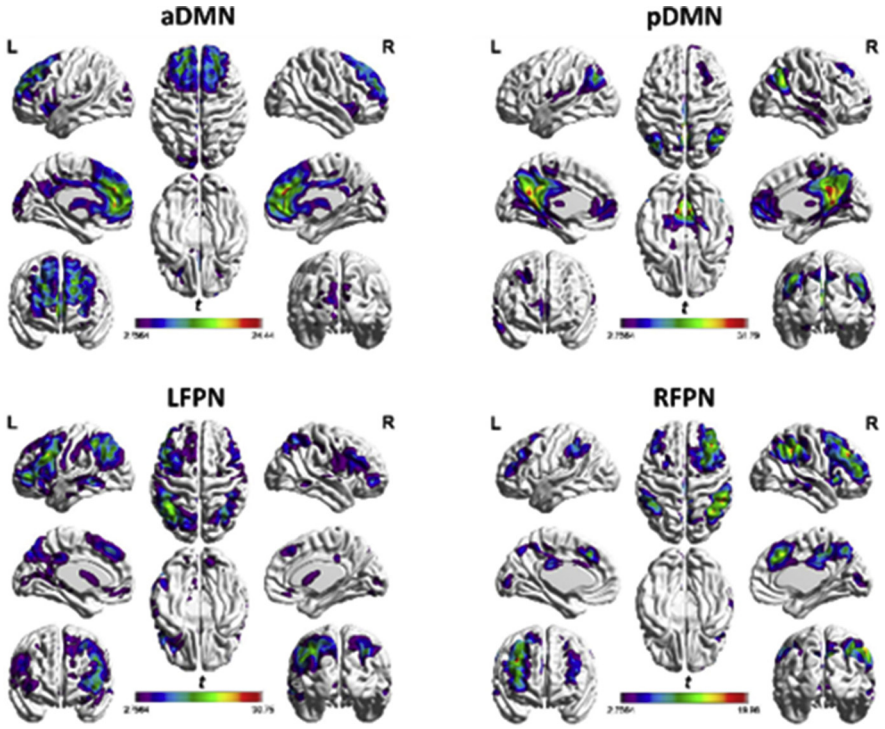

Figure 2 Cognitive implementation network through ICA screening.
One-sample *t* test of cognitive implementation network of all 30 data sets onto ICBM-152 brain surface template as identified through ICA, including anterior default mode network (aDMN), posterior default mode network (pDMN), left frontoparietal network (LFPN), and right frontoparietal network (RFPN). The *t* value (depicted by cold to warm colors) represents the spatial statistical significance of the current network. L, left; R, right.

regions with task-induced brain networks.[27] Thus, this study included exogenous afferent visual, auditory, and sensorimotor networks, as well as cognition, memory, emotion, cognitive implementation-related default networks, and fronto-parietal networks. The default mode network (DMN) is one of the resting-state networks that has the most connections. A number of studies have shown that pain of different origins and types can affect the DMN.[28—30] In particular, the medial prefrontal cortex (mPFC) and anterior cingulated cortex (ACC) comprise a major portion of the anterior default mode network (aDMN) and are involved in registering pain. Research by Baliki et al on chronic back pain, complex regional pain syndrome, and chronic pain caused by knee osteoarthritis showed that the mPFC high frequency oscillations were elevated in patients with chronic pain. The functional connectivity features for mPFC and insula were enhanced, while those of posterior DMN were reduced.[31] A study on patients with post-herpetic neuralgia using real-time fMRI neuro-feedback found that patients could adjust their pain by controlling the change rate of the ACC and blood oxygenation level dependent (BOLD) signal.[32] Medial prefrontal cortex is not only associated with peripheral afferent pain stimuli, but is also related to central pain modulation and top—down pain

Table 3 Spatial positional distributions of afferent sensory related network.

	Brodmann areas	L/R (cm^3)	Maximum *t* values (L/R) and coordinates
Somatomotor network			
Precentral gyrus	3, 4, 6, 9	20.1/20.9	18.8(−21, −12, 69)/18.3(18, −30, 63)
Postcentral gyrus	1, 2, 3, 4, 5, 6, 7, 8, 22, 40, 43, 48	26.0/23.9	19.9(−24, −39, 60)/21.1(27, −42, 69)
Supplementary motor area	4, 6, 8, 24, 32	14.0/15.3	18.3(−6, −15, 54)/20.7(6, −9, 69)
Paracentral lobule	3, 4, 5, 6	8.1/4.7	17.0(−15, −36, 63)/15.2(9, −39, 69)
Superior frontal gyrus	6, 8, 9, 10, 11, 32	15.2/18.2	18.0(−21, −9, 66)/15.4(15, −12, 69)
Middle frontal gyrus	6, 8, 9, 10, 11, 32, 44, 45, 46, 47, 48	24.5/25.3	11.1(−27, −3, 60)/12.6(33, −3, 57)
Middle cingulate gyrus	23, 24, 32	11.5/9.2	16.6(−3, −9, 48)/14.5(0, −9, 48)
Visual network			
Calcarine gyrus	17, 18, 19, 23, 30	14.7/13.9	19.0(−9, −81, 12)/18.7(3, −69, 15)
Cuneus gyrus	7, 17, 18, 19, 23	11.2/11.5	18.9(−12, −93, 30)/23.3(12, −93, 24)
Lingual gyrus	17, 18, 19, 27, 30	14.3/16.2	15.5(−21, −72, −6)/17.7(9, −69, 0)
Superior occipital gyrus	7, 17, 18, 19	10.3/10.7	23.6(−18, −93, 30)/20.1(15, −90, 24)
Middle occipital gyrus	17, 18, 19, 37, 39	19.4/12.5	15.6(−15, −96, 9)/13.0(27, −90, 15)
Fusiform gyrus	18, 19, 30, 37	6.3/8.3	17.5(−24, −72, 96)/16.4(27, −54, −6)
Audio network			
Heschl's gyrus	22, 48	1.9/1.9	21.9(−54, −9, 12)/17.4(54, −3, 6)
Superior temporal gyrus	21, 22, 38, 41, 42, 48	16.6/22.6	20.0(−60, −33, 21)/21.0(60, −3, 6)
Middle temporal gyrus	20, 21, 22, 37, 39, 41, 42, 48	24.5/18.7	11.7(−60, −42, 12)/13.1(60, −39, 12)
Postcentral gyrus	2, 3, 4, 6, 22, 43, 48	14.2/8.8	20.8(−54, −18, 15)/16.8(60, −15, 21)
Cingulate gyrus	10, 11, 23, 24, 32	22.2/19.6	17.9(−3, 18, 33)/16.3(3, 18, 33)
Insula	38, 47, 48	14.0/13.3	19.0(−39, 0, 12)/17.7(48, 3, 0)
Middle frontal gyrus	6, 8, 9, 10, 44, 45, 46	22.5/23.6	12.2(−36, 39, 18)/10.2(45, 42, 12)
Inferior frontal gyrus	6, 11, 38, 44, 45, 46, 47, 48	28.2/21.2	18.3(−51, 9, 6)/19.5(57, 15, 3)

suppression. Petrovic et al found that the placebo and opioid analgesic conditions activated ACC and the brain stem region, while the pain condition did not, suggesting that the endogenous opioid peptides of ACC exhibited analgesic effects.[33] Kucyi et al found that among patients with temporomandibular joint disorder, the degree of pain rumination, and mPFC as well as the functional connectivity between the medial thalamus and the cerebral aqueduct gray matter showed a positive correlation, confirming the top—down pain modulation function of mPFC.[34]

Increased sensitivity to pain that appears around damaged tissue sites is defined as secondary hyperalgesia, which is different from the peripheral mechanisms involved in primary hyperalgesia. Secondary hyperalgesia is a product of an overly-sensitive endogenous pain regulatory network. And mPFC is one of the core parts of this network. The network itself also reflects the fact that brain function resources are transferred from the pain matrix to the cognitive-associated brain regions while sensing pain.[35] In our study, the effect of SMN on aDMN was enhanced before tuina therapy in the intervention group. This may be associated with stimulation from chronic neck pain, which resulted in resource allocation abnormalities in a resting-state brain. It may also be related to the activation of the endogenous pain control loop.

Tuina therapy, using both soft and strong stimulatory techniques, can achieve pain reduction and stress relief through the relaxation of affected muscles, stretching of ligaments, and increasing the spinal intervertebral space. Our research showed that after tuina therapy, the influence of the sensorimotor network on the aDMN disappeared. This was most likely caused by a reduction in incoming pain signal and diminished top—down pain network intensity.

Thus, mPFC, as part of the prefrontal cortex and the limbic system, is closely related to the emotional response associated with pain, behavioral abnormalities, and the autonomic nervous system. Through studies on the brain functional connectivity at various distances in schizophrenic patients, Guo et al found the degree of aDMN short-range functional connectivity (FC) as well as the pDMN long-range FC were enhanced.[36] Research by Finke et al showed that in anti-N-methyl-D-aspartate receptor encephalitis, schizophrenia-like symptoms, such as memory loss and abnormal behavior, were correlated with reduced connection between the aDMN and the hippocampus as well as the structural changes in white matter surrounding the cingulate.[37] Studies by Perlaki et al on EEG and heart rate variability (HRV) have shown that during pain induction, only mPFC and HRV showed significant correlation; the parasympathetic component of HRV and the BOLD signal of mPFC showed positive correlation, while the sympathetic component was negatively correlated.[38] Although clinical depression was ruled out among the patients in our study, their HAMD scores decreased significantly after treatment, suggesting that tuina therapy may improve low mood, which may be related to a reversal in the causal relationship between aDMN and SMN.

This study used the resting-state networks and the afferent cognitive sensory implementation network as nodes, applied the Granger multivariate analysis, adopted the causal relationship between the GPDC-measured networks, and reached the following conclusions: compared

Table 4 Spatial positional distributions of cognitive implementation network.

	Brodmann areas	L/R (cm^3)	Maximum *t* values (L/R) and coordinates
Anterior default mode network			
Superior frontal gyrus	6, 8, 9, 10, 11, 32, 46	19.9/20.7	18.1(−21, 33, 39)/15.1(15, 60, 6)
Middle frontal gyrus	8, 9, 10, 11, 44, 45, 46, 47, 48	29.6/24.1	16.8(−24, 33, 39)/15.8(24, 51, 33)
Medial superior frontal gyrus	8, 9, 10, 11, 32	18.5/14.6	21.8(−3, 39, 30)/19.6(3, 51, 3)
Anterior cingulate gyrus	10, 11, 24, 25, 32	11.4/10.7	22.1(−9, 30, 30)/24.4(6, 42, 21)
Middle cingulate gyrus	23, 24, 32	11.0/10.7	17.6(−9, 30, 33)/18.4(6, 33, 33)
Posterior default mode network			
Middle cingulate gyrus	23	7.6/7.9	28.6(−3, −42, 36)/27.7(6, −45, 33)
Posterior cingulate gyrus	23, 26, 29, 30	3.6/2.3	29.3(0, −51, 33)/31.5(3, −45, 27)
Hippocampus	20, 27, 30, 34, 35, 37	3.9/4.2	8.1(−24, −24, −12)/12.8(30, −30, −9)
Calcarine gyrus	17, 18, 19, 23, 30	8.9/7.2	31.8(−12, −51, 6)/26.8(12, −54, 12)
Cuneus gyrus	7, 17, 18, 19, 23	7.9/7.4	25.4(−12, −57, 21)/25.7(12, −57, 21)
Lingual gyrus	17, 18, 19, 27, 30, 37	6.3/6.8	29.9(−9, −48, 3)/26.3(9, −48, 6)
Superior parietal gyrus	5, 7, 19, 40	3.3/5.9	13.1(−36, −69, 51)/7.6(36, −60, 54)
Inferior parietal gyrus	7, 39, 40	3.5/5.8	16.3()/16.0()
Angular gyrus	7, 19, 22, 39, 40, 41, 48	8.5/11.7	23.3(−42, −69, 42)/27.5(51, 60, 30)
Left frontoparietal network			
Superior frontal gyrus	6, 8, 9, 10, 11, 32	12.6/7.6	11.2(−33, 54, 0)/4.6(33, 66, 6)
Middle frontal gyrus	6, 8, 10, 11, 44, 45, 46, 47, 48	28.5/23.6	20.7(−45, 18, 39)/19.1(−42, 45, 0)
Medial superior frontal gyrus	8, 9, 10, 32	9.1/7.8	13.7(−6, 30, 48)/9.5(3, 33, 45)
Cingulate gyrus	10, 11, 23, 24, 25, 26, 29, 30, 32	13.8/15.5	9.4(−3, −33, 36)/8.9(−9, −36, 8.9)
Superior parietal gyrus	2, 5, 7, 40	11.9/7.9	18.8(−33, −66, 51)/13.5(33, −63, 51)
Inferior parietal gyrus	2, 3, 7, 39, 40	18.1/8.0	28.9(−42, −51, 51)/12.6(45, −36, 48)
Right frontoparietal network			
Superior frontal gyrus	6, 8, 9, 10, 11, 32, 46	9.8/18.3	7.5(−21, 15, 57)/12.6(21, 18, 51)
Middle frontal gyrus	6, 8, 9, 10, 11, 44, 45, 46, 47, 48	18.5/35.7	8.8(−42, 33, 36)/20.0(36, 39, 36)
Medial superior frontal gyrus	8, 9, 10, 32	14.3/7.5	16.2(0, 27, 42)/14.8(3, 24, 45)
Cingulate gyrus	10, 11, 23, 24, 25, 26, 29, 30, 32	9.5/19.3	12.0(0, 30, 36)/16.3(6, −27, 42)
Superior parietal gyrus	2, 5, 7, 40	6.9/5.7	8.3(−12, −69, 42)/12.9(42, −51, 57)
Inferior parietal gyrus	2, 7, 39, 40	−/10.4[a]	−/17.3(54, −39, 48)[a]

[a] No activated voxels on the left.

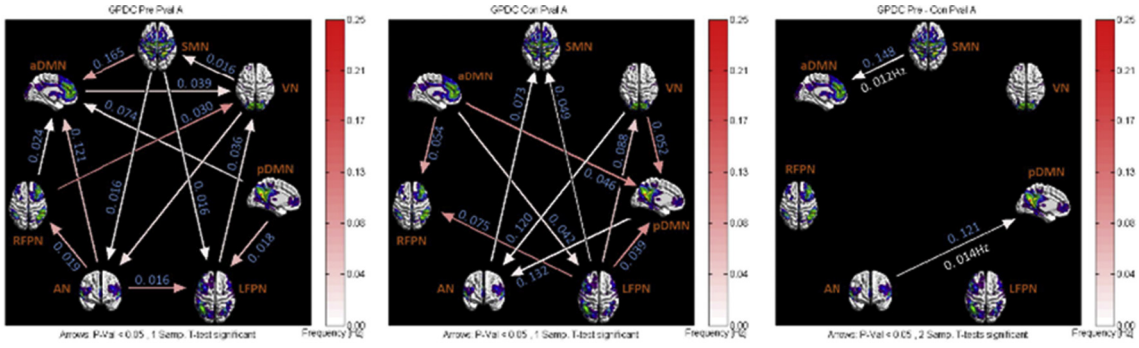

Figure 3 Inter- and intra-group comparisons of the intervention group and the control group before treatment.
Panels represent visual descriptions of causal connectivity between 2 networks among the 7 resting state networks, including sensorimotor network (SMN), visual network (VN), audio network (AN), anterior default mode network (aDMN), posterior default mode network (pDMN), left frontoparietal network (LFPN) and right frontoparietal network (RFPN). Blue numbers indicate strength of causality. Arrow directions represent cause and effect. As FNC calculated GPDC in frequency domain, values on the color bar (corresponding with arrow colors) demonstrate frequency at which causality was found. Left panel: one-sample *t* test result of inter-group intranetwork causal relationship of the intervention group before tuina therapy. Center panel: one-sample *t* test result of intergroup intranetwork causal relationship of the control group. Right panel: two-sample *t* test result of intra-group intra-network causal relationship of the intervention group minus the control group. Numbers in white represent frequencies of the causal connection.

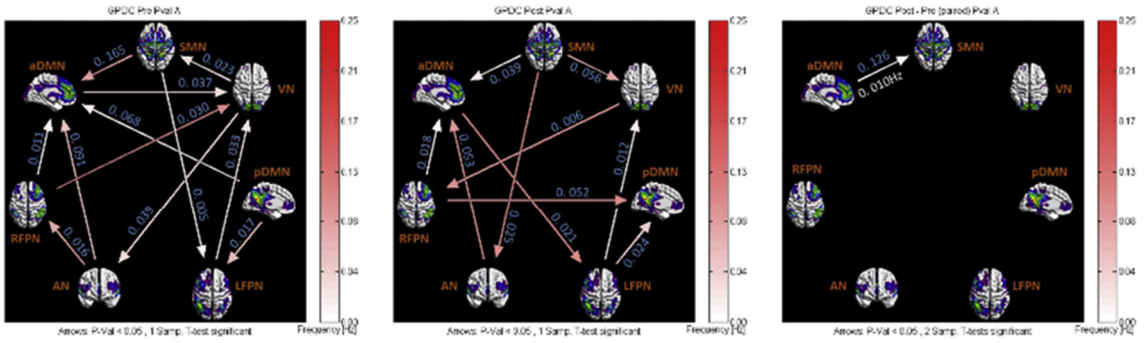

Figure 4 Inter- and intra-group comparisons of the intervention group before and after treatment.
Panels represent visual descriptions of causal connectivity between 2 networks among the 7 resting state networks, including sensorimotor network (SMN), visual network (VN), audio network (AN), anterior default mode network (aDMN), posterior default mode network (pDMN), left frontoparietal network (LFPN), and right frontoparietal network (RFPN). Blue numbers indicate strength of causality. Arrow directions represent cause and effect. As FNC calculated GPDC in frequency domain, values on the color bar (corresponding with arrow colors) demonstrate frequency at which causality was found. Left panel: one-sample *t* test result of the inter-group intra-network causal relationship after treatment. Center panel: one-sample *t* test result of the intergroup intranetwork causal relationship before treatment. Right: paired *t* test result of the intragroup intranetwork causal relationship of post-treatment minus pre-treatment.

with the control group, the influence of the sensorimotor network on the anterior default mode network was enhanced for patients with chronic cervical spondylosis, and the influence of the auditory network on the posterior default mode network was also enhanced. Following tuina therapy, the causal relationship between the sensorimotor network and the anterior default mode network was reversed compared with pre-treatment.

Limitations of this study include a relatively small patient sample, the *P*-value has not been corrected, insufficient statistical power, and nonintegration of intranetwork correlation of brain white matter fiber diffusion tensor imaging analysis. In addition to increased sample size, future studies should aim to investigate the impact of pain on brain function and brain structure from a multi-modal perspective, that is, from the resting state to the task state and from functional connectivity to structural connectivity.

Conclusion

Chinese tuina therapy not only relieves pain, but also appears to improve emotional, cognitive, and executive brain dysfunction due to pain by eliminating the influence of afferent pain on the default mode networks.

Conflict of interest

The authors have no conflicts of interest to declare.

Funding statement

This research was supported by the Young Teachers Foundation of Beijing University of Chinese Medicine, No. 2013-JYBZZ-JS-047. The funders had no role in study design, data collection and analysis, decision to publish, or preparation of the manuscript.

Author's contribution

Hua Zhang, Hong Chen, Bin Zheng, and Zhiwen Weng participated in the design of this study. Hao Wang, Duoduo Li, Baolin Jia carried out Chinese Tuina treatment and acquired the clinical data. Zhongjian Tan acquired the fMRI data. Hua Zhang analyzed and interpreted the data. Hua Zhang drafted the manuscript. Hong Chen obtained funding. Bin Zheng and Zhiwen Weng provided technical and material support. Hua Zhang and Hong Chen supervised the study.

References

1. Debono DJ, Hoeksema LJ, Hobbs RD. Caring for patients with chronic pain: pearls and pitfalls. *J Am Osteopath Assoc*. 2013; 113(8):620—627.
2. Loeser D, Butler SH, Chapman CR, Turk DC. *Bonica's Management of Pain*. 3rd ed. Philadelphia, PA: Lippincott Williams & Wilkins; 2001:18—25.
3. Fine PG. Long-term consequences of chronic pain: mounting evidence for pain as a neurological disease and parallels with other chronic disease states. *Pain Med*. 2011;12(7):996—1004.
4. Wu Z, Wu Z. *Surgery*. 6th ed. Beijing, China: People's Health Press; 2004:880—885.
5. Sun C, Wu C, Kang R, Xi D, Sun S, Ma D. *Traditional Chinese Orthopedics and Traumatology Experience of Liu Shoushan*. Beijing, China: People's Health Press; 2006:250—252.
6. Kong J, White NS, Kwong KK, et al. Using fMRI to dissociate sensory encoding from cognitive evaluation of heat pain intensity. *Hum Brain Mapp*. 2006;27(9):715—721.
7. Kim SH, Lee Y, Lee S, Mun CW. Evaluation of the effectiveness of pregabalin in alleviating pain associated with fibromyalgia: using functional magnetic resonance imaging study. *PLoS One*. 2013;8(9):e74099.
8. Barnett L, Seth AK. The MVGC multivariate Granger causality toolbox: a new approach to Granger-causal inference. *J Neurosci Methods*. 2014;223:50—68.
9. Goebel R, Roebroeck A, Kim DS, Formisano E. Investigating directed cortical interactions in time-resolved fMRI data using

vector autoregressive modeling and Granger causality mapping. *Magn Reson Imaging*. 2003;21(10):1251—1261.
10. Deshpande G, Hu X, Stilla R, Sathian K. Effective connectivity during haptic perception: a study using Granger causality analysis of functional magnetic resonance imaging data. *Neuroimage*. 2008;40(4):1807—1814.
11. Londei A, D'Ausilio A, Basso D, Belardinelli MO. A new method for detecting causality in fMRI data of cognitive processing. *Cogn Process*. 2006;7(1):42—52.
12. Demirci O, Stevens MC, Andreasen NC, et al. Investigation of relationships between fMRI brain networks in the spectral domain using ICA and Granger causality reveals distinct differences between schizophrenia patients and healthy controls. *Neuroimage*. 2009;46(2):419—431.
13. Liao W, Mantini D, Zhang Z, et al. Evaluating the effective connectivity of resting state networks using conditional Granger causality. *Biol Cybern*. 2010;102(1):57—69.
14. Havlicek M, Jan J, Brazdil M, Calhoun VD. Dynamic Granger causality based on Kalman filter for evaluation of functional network connectivity in fMRI data. *Neuroimage*. 2010;53(1):65—77.
15. Bruneau EG, Jacoby N, Saxe R. Empathic control through coordinated interaction of amygdala, theory of mind and extended pain matrix brain regions. *Neuroimage*. 2015;114:105—119.
16. Leung A, Zhao Y, Shukla S. The effect of acupuncture needle combination on central pain processing—an fMRI study. *Mol Pain*. 2014;10:23.
17. Oldfield RC. The assessment and analysis of handedness: the Edinburgh inventory. *Neuropsychologia*. 1971;9(1):97—113.
18. Li Z, Chen D, Wu D, et al. The third National Symposium Summary of cervical spondylosis. *Chin J Surg*. 2008;46(23):1796—1799.
19. Tanaka Y, Kokubu S, Sato T, et al. Results of conservative treatment for cervical radiculopathy and their prediction. *Orthop Surg Traumatol*. 1997;40:167—174.
20. Hamilton M. A rating scale for depression. *J Neurol Neurosurg Psychiatry*. 1960;23:56—62.
21. Chao-Gan Y, Yu-Feng Z. DPARSF: a MATLAB toolbox for "pipeline" data analysis of resting-state fMRI. *Front Syst Neurosci*. 2010;4:13.
22. Calhoun VD, Liu J, Adali T. A review of group ICA for fMRI data and ICA for joint inference of imaging, genetic, and ERP data. *Neuroimage*. 2009;45(suppl 1):S163—S172.
23. Jafri MJ, Pearlson GD, Stevens M, Calhoun VD. A method for functional network connectivity among spatially independent resting-state components in schizophrenia. *Neuroimage*. 2008;39(4):1666—1681.
24. Xia M, Wang J, He Y. BrainNet Viewer: a network visualization tool for human brain connectomics. *PLoS One*. 2013;8(7):e68910.
25. Allen EA, Erhardt EB, Damaraju E, et al. A baseline for the multivariate comparison of resting state networks. *Front Syst Neurosci*. 2011;5:2.
26. Mazziotta JC, Toga AW, Evans A, Fox P, Lancaster J. A probabilistic atlas of the human brain: theory and rationale for its development. The International Consortium for Brain Mapping (ICBM). *Neuroimage*. 1995;2(2):89—101.
27. Cauda F, Torta DM, Sacco K, et al. Shared "core" areas between the pain and other task-related networks. *PLoS One*. 2012;7(8):e41929.
28. Cauda F, Sacco K, Duca S, et al. Altered resting state in diabetic neuropathic pain. *PLoS One*. 2009;4(2):e4542.
29. Kucyi A, Moayedi M, Weissman-Fogel I, et al. Enhanced medial prefrontal-default mode network functional connectivity in chronic pain and its association with pain rumination. *J Neurosci*. 2014;34(11):3969—3975.
30. Sundermann B, Burgmer M, Pogatzki-Zahn E, et al. Diagnostic classification based on functional connectivity in chronic pain: model optimization in fibromyalgia and rheumatoid arthritis. *Acad Radiol*. 2014;21(3):369—377.
31. Baliki MN, Mansour AR, Baria AT, Apkarian AV. Functional reorganization of the default mode network across chronic pain conditions. *PLoS One*. 2014;9(9):e106133.
32. Guan M, Ma L, Li L, et al. Self-regulation of brain activity in patients with postherpetic neuralgia: a double-blind randomized study using real-time FMRI neurofeedback. *PLoS One*. 2015;10(4):e0123675.
33. Petrovic P, Kalso E, Petersson KM, Ingvar M. Placebo and opioid analgesia—imaging a shared neuronal network. *Science*. 2002;195(5560):1737—1740.
34. Kucyi A, Moayedi M, Weissman-Fogel I, et al. Enhanced medial prefrontal-default mode network functional connectivity in chronic pain and its association with pain rumination. *J Neurosci*. 2014;34(11):3969—3975.
35. Weaver KE, Richardson AG. Medial prefrontal cortex, secondary hyperalgesia, and the default mode network. *J Neurosci*. 2009;29(37):11424—11425.
36. Guo W, Liu F, Xiao C, et al. Increased short-range and long-range functional connectivity in first-episode, medication-naive schizophrenia at rest schizophrenia. *Schizophr Res*. 2015;166(1—3):144—150.
37. Finke C, Kopp UA, Scheel M, et al. Functional and structural brain changes in anti—N-methyl-D-aspartate receptor encephalitis. *Ann Neurol*. 2013;74(2):284—296.
38. Perlaki G, Orsi G, Schwarcz A, et al. Pain-related autonomic response is modulated by the medial prefrontal cortex: an ECG-fMRI study in men. *J Neurol Sci*. 2015;349(1—2):202—208.